

# Revisiting the Disequilibrium Issues in Tackling Heart Disease Classification Tasks

Thao Hoang<sup>1</sup>, Linh Nguyen<sup>1</sup>, Khoi Do<sup>1,\*</sup>, Duong Nguyen<sup>2</sup>, and Viet Dung Nguyen<sup>1</sup>

Hanoi University of Science and Technology, Pusan National University  
{hoangminhthao1111, nguyenphuonglinh2611, khoido8899, mduongbkhn,  
nvdung.bme, danghoanglan271}@gmail.com

**Abstract.** In the field of heart disease classification, two primary obstacles arise. Firstly, existing Electrocardiogram (ECG) datasets consistently demonstrate imbalances and biases across various modalities. Secondly, these time-series data consist of diverse lead signals, causing Convolutional Neural Networks (CNNs) to become overfitting to the one with higher power, hence diminishing the performance of the Deep Learning (DL) process. In addition, when facing an imbalanced dataset, performance from such high-dimensional data may be susceptible to overfitting. Current efforts predominantly focus on enhancing DL models by designing novel architectures, despite these evident challenges, seemingly overlooking the core issues, therefore hindering advancements in heart disease classification. To address these obstacles, our proposed approach introduces two straightforward and direct methods to enhance the classification tasks. To address the high dimensionality issue, we employ a Channel-wise Magnitude Equalizer (CME) on signal-encoded images. This approach reduces redundancy in the feature data range, highlighting changes in the dataset. Simultaneously, to counteract data imbalance, we propose the Inverted Weight Logarithmic Loss (IWL) to alleviate imbalances among the data. When applying IWL loss, the accuracy of state-of-the-art models (SOTA) increases up to 5% in the CPSC2018 dataset. CME in combination with IWL also surpasses the classification results of other baseline models from 5% to 10%.

**Keywords:** ECG Classification · Imbalanced Data · Power Variance

## 1 Introduction

In recent times, there has been a remarkable rise in the number of studies on applications of Artificial Intelligence (AI) in the healthcare field [6,24]. There are many benefits associated with this tendency, such as in the areas of disease classification [35,3,27], drug discovery [13,1] and tumor segmentation [19,10].

Subclinical diagnoses for heart disease classification mostly depend on the Electrocardiogram (ECG) signal's evolving patterns over time. 12 leads are used

---

\* Project Leader

in the acquiring process; each lead depicts a distinct view of the ECG signal. Although there exists a noticeable imbalance in magnitude amongst channels, some techniques aim to enhance outcomes by reconfiguring model [5,9,18], transfer learning [7,29,20] and employing feature extraction [17]. Nevertheless, when utilized on frequency-varied biomedical datasets, particularly ECG signals, these methods exhibit a disregard for the variance in power distribution for every ECG lead and result in an increase in model size. In low-magnitude signal channels, the model cannot extract the essential information effectively, even with feature extraction methods. In addition, not having been thoroughly investigated, the possible risks of the channel-wise imbalance would result in the AI model receiving insufficient data.

Another significant concern is that data collected in clinical settings often face challenges due to a long-tailed distribution of classes. Therefore, several methods have been developed: oversampling data [26,28], undersampling data [34], and data augmentation [32]. All mentioned approaches aim to equilibrate the distribution of classes. However, while oversampling may aid in the reduction of imbalances, it carries the danger of causing the model to become overfit to long-tailed classes. Undersampling, on the other hand, risks losing vital information, potentially limiting the model’s ability to generalize to new data. Meanwhile, data augmentation can inadvertently augment the class imbalances by generating more samples from undesired classes [33].

This paper aims to address the previously mentioned issues with the ECG dataset. First, a thorough empirical investigation into each channel’s variation is carried out to obtain a greater understanding of the differences between the signal leads. Taking note of each lead’s diminishing distribution and signal power, we propose a Channel-wise Magnitude Equalizer (CME) (see Fig. 1) method. In order to preserve the frequency characteristics while also improving the information of the fading signal, we normalized the data and used time-frequency interpolation. Through this process, the power of acquired data is equalized with that of raw data. Second, we propose the Inverted Weight Logarithmic (IWL) loss function to tackle class imbalance issue without complicating AI models. In summary, our main contributions to this paper are as follows:

- A thorough empirical study is undertaken on variations in ECG leads in order to gain a profound insight into the fundamental properties of the signal.
- Propose CME method to address power imbalances and distribution variation in fading signals, and improve the potential information contained while preserving the signal frequency characteristics.
- Propose IWL loss function to tackle the data distribution imbalance problem.
- Experiment to verify the efficacy of our suggested method by equitably contrasting it with multiple baselines. Besides, an ablation test to evaluate the method’s adaptability is also taken into account.

## 2 Methodology

The flow of the proposed methodology is presented in Fig. 1.

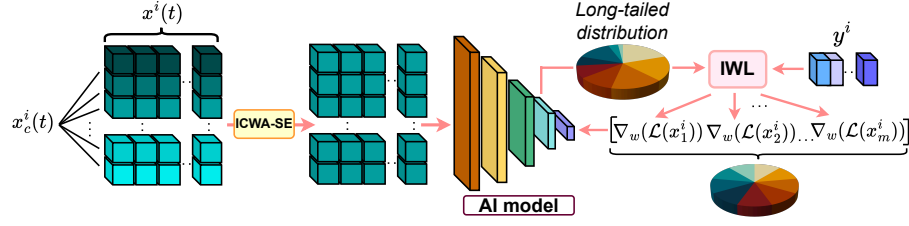


Fig. 1: Methodology Overview: The input channel-wise ECG signal first goes through the CME process. Here, we normalize each channel-wise signal and assess its contribution (illustrated by different tones of green color) to the loss update by using an Attention-like layer. The  $C$  channels are then squeezed and excited based on their relative importance, followed by an interpolation. The obtained images are then fed to the AI model. The original dataset has a long-tailed distribution. After each training epoch, the model gives prediction vectors, and together with true labels  $y^i$ , they go into the IWL loss function. Here, IWL loss performs gradient balancing and updates to the AI model to strengthen the weight from long-tailed classes and weaken the data from high-frequency classes.

## 2.1 Preliminary and Notations

Given a dataset containing  $N$  samples represented as  $\{\mathbf{x}^i, \mathbf{y}^i\}_i^N$  with the total of  $M \sim p(M)$  classes, each sample belonging to class  $m$  is represented as  $(\mathbf{x}_m^i, \mathbf{y}_m^i)$ , where  $m \in [1, \dots, M]$ . We defined the model's weight as  $\theta$ , and the purpose is to minimize the loss function  $\mathcal{L}$ . For instance,

$$\min_{\theta} \mathcal{L}(\theta) \triangleq \mathbb{E}_{\mathbf{x}^i, \mathbf{y}^i \sim P(\mathbf{x}, \mathbf{y})} [\ell(\mathbf{x}^i, \mathbf{y}^i | \theta)]. \quad (1)$$

Noted that the main consideration can be perceived as a classification task, we reshape the problem as presented in (2):

$$\min_{\theta} \mathcal{L}(\theta) = \frac{1}{N} \frac{1}{M} \sum_{i=1}^N \sum_{m=1}^M [\ell(\mathbf{x}_i^m, \mathbf{y}_i^m | \theta)], \quad (2)$$

with  $\mathcal{L}(\theta)$  is the cross entropy function, and can be represented as follows:

$$\mathcal{L}(\mathbf{x}^i, \mathbf{y}^i) = - \sum_{m=0}^{M-1} \log \left( \frac{\exp\{f_{\theta}(\mathbf{x}_m^i)\}}{\sum_{m'=0}^{M-1} \exp\{f_{\theta}(\mathbf{x}_{m'}^i)\}} \right) \mathbf{y}_m^i \quad (3)$$

with  $f_{\theta}(\cdot)$  is the classification task of the given AI model.

## 2.2 Empirical Study

To achieve a comprehensive illustration of the uncovered problems, we take a deep analysis of the data (refer to Fig. 2a), where the input data  $\mathbf{x}^i \in \mathbb{R}^{C \times L}$

is considered as a composition of multiple stochastic random processes  $x_c^i(t)$ , where  $C, L$  is the number of channels and channel signal length. Easily seen from Fig. 2a, the primary issue while learning patterns from the dataset is that the maximum level of each channel varies significantly. Consequently, a magnitude gap exists between learning gradients due to the fact that the input channels with higher magnitudes will contribute to the higher loss value. For instance:

$$\begin{aligned} \mathcal{L}(\mathbf{x}^i, \mathbf{y}^i) &= - \sum_{i=0}^{N-1} \sum_{m=0}^{M-1} \sum_{c=0}^{C-1} \log \left( \frac{\exp\{f_\theta(\mathbf{x}_{m,c}^i)\}}{\sum_{m'=0}^{M-1} \exp\{f_\theta(\mathbf{x}_{m',c}^i)\}} \right) \mathbf{y}_{m,c}^i \\ &= - \sum_{i=0}^{N-1} \sum_{m=0}^{M-1} \sum_{c=0}^{C-1} \log \left( \frac{\exp\{f_\theta(\beta_{m,c} \bar{\mathbf{x}}_{m,c}^i)\}}{\sum_{m'=0}^{M-1} \exp\{f_\theta(\beta_{m',c} \bar{\mathbf{x}}_{m',c}^i)\}} \right) \mathbf{y}_{m,c}^i \\ &= - \sum_{i=0}^{N-1} \sum_{m=0}^{M-1} \sum_{c=0}^{C-1} \beta_{m,c} \log \left( \frac{\exp\{f_\theta(\bar{\mathbf{x}}_{m,c}^i)\}}{\sum_{m'=0}^{M-1} \exp\{f_\theta(\beta_{m',c} \bar{\mathbf{x}}_{m',c}^i)\}} \right) \mathbf{y}_{m,c}^i, \quad (4) \end{aligned}$$

where  $\bar{\mathbf{x}}_{m,c}^i, \beta_{m,c}$  represents the normalized signal of data  $\mathbf{x}^i$  and the magnitude scale according to class  $m$  and channel  $c$ , respectively. As easily seen from Equation (4), the loss will vary significantly according to different leads' power levels. Moreover, due to the nature of the ECG sampling process, there occasionally occurs an unstable power level in one lead. Thus, conventional normalization is unable to mitigate the inconsistent and imbalanced issues in ECG classification.

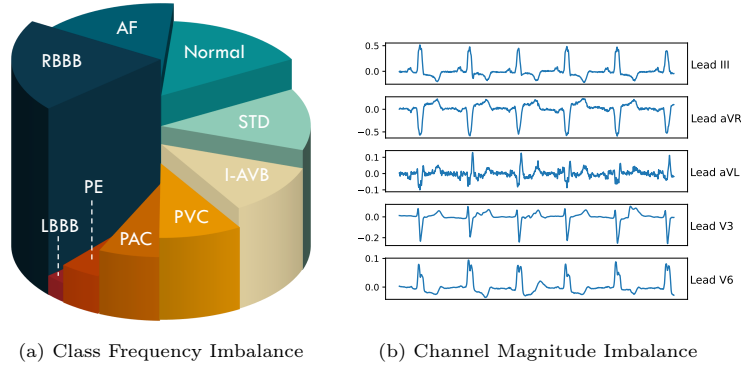


Fig. 2: Dataset illustration: a) The sampling distribution of 9 classes (total of 6400 single label samples): Right bundle branch block (RBBB), Atrial fibrillation (AF), Normal, ST-segment depression (STD), First-degree atrioventricular block (I-AVB), Premature ventricular contraction (PVC), Premature atrial contraction (PAC), ST-segment elevated (STE) and Left bundle branch block (LBBB). b) The ECG waveforms (Left bundle branch block disease, from A0011). There are 5 leads being illustrated.

### 2.3 Squeeze and Excitation with Channel-wise Magnitude Equalizer

From the comment in Section 2.2, we proposed a simple method for our model architecture’s first layer (Fig. 1). We used an Attention-like layer [25] to quantify the contribution of each channel to the loss update. The SE approach from [12] is then used to scale each channel based on its relative relevance.

Instead of the traditional structure, we applied an inverted version, CME. Our goal is to excite the channels with lower loss update contribution and squeeze the channels with higher contribution, i.e. as follows:

$$k_c^i = F_{\text{CME}}(z_{\cdot,c}^i) = \frac{e^{-\|\mathbf{x}_{\cdot,c}^i\|}}{\sum_{c'=0}^{C-1} e^{-\|\mathbf{x}_{\cdot,c'}^i\|}}, \quad (5)$$

where  $k_c^i$  represents the squeeze and excitation factor according to channel  $c$ . Applying all channels through the input data  $\mathbf{x}_c^i$ , we have the set of factor  $k = \{k_c^i \mid c = 1, 2, \dots, C\}$ . Subsequently, we leverage the SE factor to scale the channel-wise representation  $\mathbf{z}_{\text{SE}}^i$  as follows:

$$\mathbf{z}_{\text{SE}}^i = F_{\text{scale}}(\mathbf{x}^i, k), \quad (6)$$

where  $F_{\text{scale}}(\cdot, \cdot)$  is the Hadamard product function, represented as follows:

$$F_{\text{scale}}(x, k) = x \cdot k. \quad (7)$$

By doing this step, the channel-wise signal, i.e., leads, are automatically squeezed and excited according to the instantaneous signal. To this end, these scaled signals are interpolated to not just enhance the quality of information but also keep the frequency properties unchanged. Note that, this CME block is a hyperparameter-free approach that equalizes the gradient magnitude across tasks to encourage learning low power  $\mathcal{P}(x_c^i(t)) = \frac{1}{T} \sum_{t=0}^{T-1} \|x_c^i(t)\|$  signal and difference in signal distribution among channel ( $p(x_h^i) \neq p(x_k^i), \forall h \neq k$ ).

### 2.4 Equalized Scalarization via IWL Loss

As mentioned in the previous sections, data imbalance is a critical issue in learning biomedical data in general and ECG classification in particular. To tackle the problem efficiently, we proposed a new loss function which is IWL (Inverted Weight Logarithmic) loss to deal with a long-tailed dataset:

$$\mathcal{L} = -\frac{1}{N} \sum_{i=0}^{N-1} \sum_{m=0}^{M-1} \left( \log \left( \frac{10}{p(\hat{x}_m^i) + \varepsilon} \right) \right)^\beta \log(p(\hat{x}_m^i)) y_m^i, \quad (8)$$

where  $p(\hat{x}_m^i) \in \mathbb{R} = \exp\{\hat{x}_m^i\} / \sum_{m'=0}^{M-1} \exp\{\hat{x}_{m'}^i\}$  is the normalized prediction vector and  $\hat{x}_m^i = f_{\mathcal{W}}(x_m^i)$ , respectively.  $\varepsilon$  is an infinitesimal and  $\beta$  is temperature parameter. IWL can put a higher weight onto the low confidence logits while keeping a small weight for well-classified ones. This feature makes the model focus more on classifying long-tailed rare categories and avoid forgetting high confidence classes, compared to Focal[14] or CBFocal[8].

### 3 Experimental Evaluation

#### 3.1 Experimental Settings

**Problems.** We conduct three large experiments (see Table 1). First, we reimplement state-of-the-art models and techniques that use the same dataset as ours, which include: Auto Encoder [17], 1D DNN [5], BiRNN [16], BiLSTM [21], Transformer [4], ResNet [11], and augmentation. Besides, we replace the loss function used in those models in the first experiment with our IWL loss and compare the results obtained from two loss functions. Second, we apply different loss functions to our ICWA-SE trained by EfficientNetB0, which are: CB Focal [8], Class-balanced [8], Focal [14] and LDAM [2] loss which are SOTA loss functions that popularly used for imbalanced dataset. In each loss, we utilize the best hyperparameters that are justified by their authors. Third, we conduct some model architectures (RegNet [31], ResNeXt [30], EfficientNetV2 [23]) combined with our proposed ICWA-SE and IWL loss function.

For ours IWL loss, we provide a configuration with ten different values of  $\beta \in \{0.1, 0.3, 0.5, 0.7, 0.9, 1, 2, 3, 4, 5\}$  to find the optimal one (see Section 3.3).

**Datasets.** To evaluate the performance of the proposed methods, we make use of the CPSC2018 dataset [15], the dataset consists of 6877 12-lead ECG recordings sampled at 500Hz, each recording has a length from 6s to 60s. However, as there exist several samples with multiple labels, in our experiments, only 6400 samples with single labels will be used to avoid conflicted patterns between multi-label samples and single-label samples. We then split the obtained dataset into the training set, and test set by the ratio [0.9, 0.1], respectively. For the ICWA-SE method, after cutting off 500 data points at the beginning (to prevent the artifact from the first second of the acquisition process), only 2500 data points from each sample were used for implementation. Since the shortest samples from the dataset have a length of 3000 data points (equivalent to 6s at 500Hz sampling rate), we only use the first 3000 data points of all datasets to avoid differences in the size of the input.

To deeply evaluate our proposed method with imbalanced data, we shuffle the dataset using the following equation  $N = \max(x_m^i) * \alpha^{(m/(M-1))}$  with  $\alpha \in \{0.05, 0.01\}$ , note  $\alpha$  as a parameter represent the imbalance dataset, the smaller the  $\alpha$  value, the more imbalance the data is,  $\alpha = 0.05$  claims the distribution of the original dataset.

**Experiment setup and Evaluation metrics.** We conduct experiments on 2D CNN models that are mentioned above. The data was trained over 150 epochs with learning rate equals 0.001 and Adam optimizer. The batch size is set to 64. Two metrics accuracy (%) and F1-score (%) are used for performance evaluation.

#### 3.2 Overall Performance

Table 1 shows the results of all experiments that we mentioned in Section 3.1. Overall, the highest accuracy and F1-score are achieved with our method, which outperforms others in both  $\alpha$  values. In most experiments, it’s observed that

the outcomes from the original dataset surpass those obtained with smaller  $\alpha$  values. However, the performance of the ICWA-SE model with the IWL loss demonstrates a contrary trend, where the superior outcome is achieved with the dataset possessing a smaller imbalanced factor ( $\alpha = 0.01$ ). This suggests the capability of our proposed method to handle highly imbalanced data effectively.

**Comparison to State-of-the-art models.** We bring into comparison four SOTA models using two loss functions, Cross-Entropy loss and our IWL loss. From Table 1, it is noticeable that the accuracies of most SOTA models with IWL loss are higher compared to those without its adoption (from 0.5% to 5%), which can prove the effectiveness of our IWL loss function.

**Comparison to State-of-the-art loss functions.** To examine the combination of the IWL loss when being applied on CME method, five SOTA loss functions have been used for comparison (trained with EfficientNetB0 model). The obtained results with four loss functions are higher than all the reimplemented SOTA models (except for CB Focal loss), proving the efficiency of our CME method. It is also noted that our IWL loss function give the best results on the proposed CME method compare with the other five loss functions used, which can prove the effectiveness combination of CME method and IWL loss.

Table 1: Comparison of our proposed model with other models over two alpha values. Each method is tested with two scenarios including  $\alpha = 0.05$ , which is the original dataset, and  $\alpha = 0.01$  whose imbalance among classes is stronger. The results that obtained using our CME and IWL loss is bolded to denote that our methods outperform others in experiment.

Method	Loss	$\alpha = 0.05$ (Original)		$\alpha = 0.01$	
		Accuracy	F1-score	Accuracy	F1-score
(1D) Auto Encoder [17]	Cross-Entropy	67.8 $\pm$ 1.2	58.0 $\pm$ 1.6	67.9 $\pm$ 1.1	59.5 $\pm$ 1.3
(1D) DNN [5]		73.0 $\pm$ 1.5	48.7 $\pm$ 1.6	71.7 $\pm$ 1.4	44.2 $\pm$ 1.1
(1D) BiRNN [16]		-	74.2	-	-
(1D) BiLSTM [21]		-	75.1	-	-
(1D) Transformer [4]		-	78.6	-	-
(1D) ResNet [11]		77.0 $\pm$ 1.5	74.3 $\pm$ 1.7	75.6 $\pm$ 1.6	68.5 $\pm$ 1.9
(1D) ResNet [11] + Aug		45.3 $\pm$ 0.2	37.0 $\pm$ 0.6	45.6 $\pm$ 0.2	37.2 $\pm$ 0.5
(1D) Auto Encoder [17]	IWL (Ours)	<b>69.1</b> $\pm$ 0.9	57.4 $\pm$ 1.2	<b>69.2</b> $\pm$ 1.1	55.6 $\pm$ 1.3
(1D) DNN [5]		<b>77.0</b> $\pm$ 0.6	<b>62.8</b> $\pm$ 0.9	<b>72.5</b> $\pm$ 0.9	<b>55.8</b> $\pm$ 1.1
(1D) ResNet [11]		<b>77.8</b> $\pm$ 0.6	67.0 $\pm$ 1.0	<b>80.7</b> $\pm$ 0.7	<b>70.1</b> $\pm$ 0.8
(1D) ResNet [11] + Aug		<b>45.8</b> $\pm$ 0.2	<b>37.5</b> $\pm$ 0.5	<b>45.9</b> $\pm$ 0.2	<b>37.4</b> $\pm$ 0.5
(2D) EfficientNetB0 [22] + CME (Ours)	CB Focal [8] ( $\gamma = 2$ )	24.2 $\pm$ 0.2	8.1 $\pm$ 0.1	24.0 $\pm$ 0.3	10.1 $\pm$ 0.1
	Class-balanced [8]	80.8 $\pm$ 0.1	74.9 $\pm$ 0.2	80.7 $\pm$ 0.3	74.0 $\pm$ 0.4
	Focal [14] ( $\gamma = 2$ )	81.8 $\pm$ 0.3	73.2 $\pm$ 0.6	81.2 $\pm$ 0.2	71.5 $\pm$ 0.3
	LDAM [2] ( $\mu = 0.2, s = 20$ )	79.9 $\pm$ 0.9	73.8 $\pm$ 0.6	78.7 $\pm$ 0.7	72.1 $\pm$ 0.5
	Cross-Entropy	78.1 $\pm$ 0.7	69.4 $\pm$ 1.0	77.5 $\pm$ 0.8	70.3 $\pm$ 1.1
(2D) RegNet [31] + CME	IWL (Ours)	77.5 $\pm$ 1.1	71.6 $\pm$ 1.9	80.0 $\pm$ 0.8	71.1 $\pm$ 1.1
(2D) ResNeXt [11] + CME		78.2 $\pm$ 0.7	71.2 $\pm$ 0.8	79.1 $\pm$ 0.4	70.9 $\pm$ 0.9
(2D) EfficientNetV2 [23] + CME		81.9 $\pm$ 0.5	72.5 $\pm$ 0.6	81.7 $\pm$ 0.5	72.9 $\pm$ 0.8
(2D) EfficientNetB0 [22] + CME + IWL loss		<b>83.2</b> $\pm$ 0.6	<b>79.1</b> $\pm$ 0.8	<b>85.2</b> $\pm$ 0.7	<b>81.0</b> $\pm$ 0.8
		$\uparrow$ 1.3	$\uparrow$ 4.2	$\uparrow$ 3.5	$\uparrow$ 8.1

### 3.3 Ablation Test

**Configurations of  $\beta$ .** The  $\beta$  value of the IWL loss function is examined to obtain the optimal one for the model performance. Table 2 shows the results of the experiment carried out with two models: ResNet and ICWA-SE, each involves the IWL loss function with 10 different values of  $\beta \in \{0.1, 0.3, 0.5, 0.7, 0.9, 1, 2, 3, 4, 5\}$ . It can be seen that the results obtained with different  $\beta$  values fluctuated, however, the smaller  $\beta$  values give better performances. For the ResNet model,  $\beta = 0.1$  gives better accuracy than all other results with  $\alpha = 0.5$ , and  $\beta = 0.3$  gives the best accuracy with the data whose imbalance factor  $\alpha = 0.1$ . For ICWA-SE, the best result in both  $\alpha$  values was acquired when  $\beta = 0.3$ , both in accuracy and F1-score. The higher  $\beta$  values do not improve the performance of the two models, therefore,  $\beta = 0.3$  has been used when implementing IWL to other methods for comparison.

Table 2: Quantitative results obtain from experiments with different  $\beta$  values.

$\beta$	$\alpha = 0.05$ (Original)				$\alpha = 0.01$			
	ResNet		CME		ResNet		CME	
	Accuracy	F1-score	Accuracy	F1-score	Accuracy	F1-score	Accuracy	F1-score
0.1	80.5 $\pm$ 0.5	72.4 $\pm$ 0.5	81.6 $\pm$ 0.5	73.4 $\pm$ 0.5	79.8 $\pm$ 0.9	70.4 $\pm$ 0.9	82.5 $\pm$ 0.6	75.0 $\pm$ 0.6
0.3	77.8 $\pm$ 0.6	67.0 $\pm$ 1.0	83.2 $\pm$ 0.6	79.1 $\pm$ 0.8	80.7 $\pm$ 0.7	70.1 $\pm$ 0.8	85.2 $\pm$ 0.7	81.0 $\pm$ 0.8
0.5	76.0 $\pm$ 0.6	65.5 $\pm$ 0.6	82.5 $\pm$ 0.7	78.1 $\pm$ 0.8	77.7 $\pm$ 1.0	70.8 $\pm$ 1.0	83.6 $\pm$ 1.0	77.0 $\pm$ 0.7
0.7	77.6 $\pm$ 0.7	71.2 $\pm$ 0.9	81.9 $\pm$ 0.5	73.5 $\pm$ 0.5	79.4 $\pm$ 0.6	66.3 $\pm$ 0.5	83.0 $\pm$ 0.6	75.2 $\pm$ 0.5
0.9	80.1 $\pm$ 0.5	71.3 $\pm$ 0.7	83.4 $\pm$ 0.7	75.0 $\pm$ 0.6	77.3 $\pm$ 0.6	73.3 $\pm$ 0.6	83.5 $\pm$ 0.7	79.2 $\pm$ 0.7
1	79.4 $\pm$ 0.8	74.5 $\pm$ 0.9	82.9 $\pm$ 0.8	76.0 $\pm$ 0.8	78.7 $\pm$ 1.0	69.9 $\pm$ 0.9	83.2 $\pm$ 0.6	78.5 $\pm$ 0.8
2	78.1 $\pm$ 0.8	71.0 $\pm$ 0.9	83.1 $\pm$ 1.1	77.3 $\pm$ 0.9	77.6 $\pm$ 1.0	71.9 $\pm$ 1.1	82.8 $\pm$ 0.9	74.9 $\pm$ 1.1
3	78.6 $\pm$ 1.0	71.3 $\pm$ 1.1	82.4 $\pm$ 1.1	75.0 $\pm$ 0.8	78.9 $\pm$ 0.9	70.6 $\pm$ 1.0	80.9 $\pm$ 1.0	77.2 $\pm$ 1.0
4	75.0 $\pm$ 1.2	60.2 $\pm$ 1.2	81.0 $\pm$ 1.0	74.6 $\pm$ 1.1	74.6 $\pm$ 1.2	64.2 $\pm$ 1.1	79.8 $\pm$ 1.0	76.4 $\pm$ 1.1
5	76.6 $\pm$ 1.3	61.8 $\pm$ 1.3	81.8 $\pm$ 1.4	75.7 $\pm$ 1.3	72.3 $\pm$ 1.5	57.5 $\pm$ 1.2	80.7 $\pm$ 0.9	76.0 $\pm$ 0.9

**Adaptability to Model Architecture Design.** To test the ability to adapt to different models of the proposed CME and IWL loss ( $\beta = 0.3$ ), four models which are RegNet [31], ResNeXt [30], EfficientNetB0 [22] and EfficientNetV2 [23] were brought to discussion. The results are presented in Table 1. As easily seen, these models give higher accuracy than all SOTA models, which is a certain proof of the adaptation of the CME method and IWL loss. The proposed method has the best performance when the EfficientNetB0 model architecture is applied.

## 4 Conclusion

In conclusion, there are some complications inhibiting the performance in ECG classification task of DL models, in particular, long-tailed class distribution, biases and multi-channel temporal data. Current endeavors primarily emphasize the enhancement of DL architectures, whereas our proposed method offers a



straightforward yet potent approach to directly confront these challenges. Utilizing the proposed CME technique on channel-wise signals effectively deals with dimensional diversity by minimizing redundant information and improving the focus on data features. Moreover, we introduce IWL loss to effectively mitigate imbalances within ECG datasets, resulting in improved classification accuracy. When applying IWL loss, the accuracy of state-of-the-art models (SOTA) increase up to 5% in the CPSC2018 dataset. CME in combination with IWL also surpasses the classification results of other baseline models from 5% to 10%.

## References

1. Abdelkrim, A., Bouramoul, A., Zenbout, I.: Machine learning methods in drug discovery: A selective review. In: 2021 International Conference on Theoretical and Applicative Aspects of Computer Science (ICTAACS) (2021)
2. Cao, K., Wei, C., Gaidon, A., Archiga, N., Ma, T.: Learning imbalanced datasets with label-distribution-aware margin loss. *Advances in neural information processing systems* (2019)
3. Caseneuve, G., Valova, I., LeBlanc, N., Thibodeau, M.: Chest x-ray image preprocessing for disease classification. *Procedia Computer Science* (2021)
4. Che, C., Zhang, P., Zhu, M., Qu, Y., Jin, B.: Constrained transformer network for eeg signal processing and arrhythmia classification. *BMC Medical Informatics and Decision Making* (2021)
5. Chen, C.Y., Lin, Y.T., Lee, S.J., Tsai, W.C., Huang, T.C., Liu, Y.H., Cheng, M.C., Dai, C.Y.: Automated eeg classification based on 1d deep learning network. *Methods* (2021)
6. Chen, J., Zheng, X., Yu, H., Chen, D.Z., Wu, J.: Electrocardio panorama: Synthesizing new eeg views with self-supervision. In: *Proceedings of the Thirtieth International Joint Conference on Artificial Intelligence, IJCAI-21*. International Joint Conferences on Artificial Intelligence Organization (2021)
7. Chu, P., Bian, X., Liu, S., Ling, H.: Feature Space Augmentation for Long-Tailed Data (2020)
8. Cui, Y., Jia, M., Lin, T.Y., Song, Y., Belongie, S.: Class-balanced loss based on effective number of samples. In: 2019 IEEE/CVF Conference on Computer Vision and Pattern Recognition (CVPR) (2019)
9. Dong, Y., Zhang, M., Qiu, L., Wang, L., Yu, Y.: An arrhythmia classification model based on vision transformer with deformable attention. *Micromachines* (2023)
10. Habib, H., Mehmood, A., Nazir, T., Nawaz, M., Masood, M., Mahum, R.: Brain tumor segmentation and classification using machine learning. In: 2021 International Conference on Applied and Engineering Mathematics (ICAEM) (2021)
11. He, K., Zhang, X., Ren, S., Sun, J.: Deep residual learning for image recognition. In: 2016 IEEE Conference on Computer Vision and Pattern Recognition (CVPR) (2016)
12. Hu, J., Shen, L., Sun, G.: Squeeze-and-excitation networks. In: 2018 IEEE/CVF Conference on Computer Vision and Pattern Recognition (2018)
13. Hu, W., Liu, Y., Chen, X., Chai, W., Chen, H., Wang, H., Wang, G.: Deep learning methods for small molecule drug discovery: A survey. *IEEE Transactions on Artificial Intelligence* (2023)
14. Lin, T.Y., Goyal, P., Girshick, R., He, K., Dollár, P.: Focal loss for dense object detection. *IEEE Transactions on Pattern Analysis and Machine Intelligence* (2020)

15. Liu, F.F., Liu\*, C.Y., Zhao, L.N., Zhang, X.Y., Wu, X.L., Xu, X.Y., Liu, Y.L., Ma, C.Y., Wei, S.S., He, Z.Q., Li, J.Q., Kwee, N.Y.: *Journal of Medical Imaging and Health Informatics* (2018)
16. Mostayed, A., Luo, J., Shu, X., Wee, W.: Classification of 12-lead ECG signals with bi-directional LSTM network. *CoRR* (2018)
17. Nijaguna, G.S., Lal, N.D., Divakarachari, P.B., Prado, R.P.d., Woźniak, M., Patra, R.K.: Feature selection using selective opposition based artificial rabbits optimization for arrhythmia classification on internet of medical things environment. *IEEE Access* (2023)
18. Qin, L., Xie, Y., Liu, X., Yuan, X., Wang, H.: An end-to-end 12-leading electrocardiogram diagnosis system based on deformable convolutional neural network with good antinoise ability. *IEEE Transactions on Instrumentation and Measurement* (2021)
19. Ranjbarzadeh, R., Bagherian Kasgari, A., Jafarzadeh Ghoushchi, S., Anari, S., Naseri, M., Bendechange, M.: Brain tumor segmentation based on deep learning and an attention mechanism using MRI multi-modalities brain images. *Sci. Rep.* (2021)
20. Saini, M., Susan, S.: Vggin-net: Deep transfer network for imbalanced breast cancer dataset. *IEEE/ACM Transactions on Computational Biology and Bioinformatics* (2023)
21. Sergey Ioffe, C.S.: Batch normalization: Accelerating deep network training by reducing internal covariate shift. *CoRR* (2015)
22. Tan, M., Le, Q.V.: Efficientnet: Rethinking model scaling for convolutional neural networks (2020)
23. Tan, M., Le, Q.V.: Efficientnetv2: Smaller models and faster training (2021)
24. Tan, Q., Ye, M., Wong, G.L.H., Yuen, P.: Cooperative joint attentive network for patient outcome prediction on irregular multi-rate multivariate health data. In: *Proceedings of the Thirtieth International Joint Conference on Artificial Intelligence, IJCAI-21. International Joint Conferences on Artificial Intelligence Organization* (2021)
25. Vaswani, A., Shazeer, N., Parmar, N., Uszkoreit, J., Jones, L., Gomez, A.N., Kaiser, L.u., Polosukhin, I.: Attention is all you need. In: *Advances in Neural Information Processing Systems. Curran Associates, Inc.* (2017)
26. Wang, S., Dai, Y., Shen, J., Xuan, J.: Research on expansion and classification of imbalanced data based on smote algorithm. *Scientific Reports* (2021)
27. Wang, X., Peng, Y., Lu, L., Lu, Z., Bagheri, M., Summers, R.M.: Chestx-ray8: Hospital-scale chest x-ray database and benchmarks on weakly-supervised classification and localization of common thorax diseases. In: *2017 IEEE Conference on Computer Vision and Pattern Recognition (CVPR)* (2017)
28. Wang, X., Xu, J., Zeng, T., Jing, L.: Local distribution-based adaptive minority oversampling for imbalanced data classification. *Neurocomputing* (2020)
29. Weimann, K., Conrad, T.O.F.: Transfer learning for ecg classification. *Scientific Reports* (2021)
30. Xie, S., Girshick, R., Dollár, P., Tu, Z., He, K.: Aggregated residual transformations for deep neural networks. In: *2017 IEEE Conference on Computer Vision and Pattern Recognition (CVPR)* (2017)
31. Xu, J., Pan, Y., Pan, X., Hoi, S., Yi, Z., Xu, Z.: Regnet: Self-regulated network for image classification. *IEEE Transactions on Neural Networks and Learning Systems* (2023)

32. Zang, Y., Huang, C., Change Loy, C.: Fasa: Feature augmentation and sampling adaptation for long-tailed instance segmentation. In: 2021 IEEE/CVF International Conference on Computer Vision (ICCV) (2021)
33. Zhang, Y., Kang, B., Hooi, B., Yan, S., Feng, J.: Deep long-tailed learning: A survey. *IEEE TRANSACTIONS ON PATTERN ANALYSIS AND MACHINE INTELLIGENCE* (2021)
34. Zhou, B., Cui, Q., Wei, X.S., Chen, Z.M.: BBN: Bilateral-branch network with cumulative learning for long-tailed visual recognition (2020)
35. Zhou, Y., He, X., Huang, L., Liu, L., Zhu, F., Cui, S., Shao, L.: Collaborative learning of semi-supervised segmentation and classification for medical images. In: 2019 IEEE/CVF Conference on Computer Vision and Pattern Recognition (CVPR) (2019)